In: DNA Adducts: Formation, Detection and Mutagenesis ISBN: 978-1-60741-433-9
Editors: E. Alvarez, R. Cunha, pp. 143-153

Chapter VII

Potency of Air Pollutants at DNA Adduct Formation and Assessment by *In Vivo* Mutagenesis

Yasunobu Aoki, Akiko H. Hashimoto, Hiromi Sato and Michi Matsumoto
National Institute for Environmental Studies, Research Center for Environmental Risk
16-2 Onogawa, Tsukuba, Ibaraki 305-8506 Japan.

Abstract

Various mutagenic polycyclic aromatic hydrocarbons (PAHs) including nitro-PAHs, associated with suspended particulate matter (SPM), are possibly deposited in the lungs and other organs of residents in urban areas. To assess the mutagenicity of air pollution and its carcinogenic risk in the lung and other organs, it is necessary to assess the genotoxicity *in vivo* of the various PAHs and nitro-PAHs in urban air. In this chapter, we review the genotoxicity, such as DNA adduct formation, of air pollutants and its assessment by *in vivo* mutagenesis.

Abbreviations

PAHs	polycyclic aromatic hydrocarbons
BaP	benzo[a]pyrene
SPM	suspended particulate matter
$PM_{2.5}$ and PM_{10}	SPM < 2.5 and 10 μm diameter, respectively
DNP	dinitropyrene
3NBA	3-nitrobenzanthrone
DEP	diesel exhaust particle
BPDE	benzo[a]pyrene diol-epoxide
RAL	relative adduct level

WBCs	white blood cells
DE	diesel engine exhaust
MF	mutant frequency

1. Introduction: Mutagenic PAHs in Urban Air

PAHs and nitro-PAHs are generated by the combustion of fossil fuels and are found in diesel and boiler exhaust. Many PAHs are recognized as mutagens and carcinogens, and are associated with SPM in ambient air. SPM < 2.5 μm in diameter ($PM_{2.5}$) tends to be easily trapped in pulmonary bronchia, where it possibly induces mutations that lead to tumor formation. Benzo[a]pyrene (BaP) is a typical environmental pollutant contained in SPM. Its mutagenic potency has been well examined by means of *in vitro* assay systems, such as the Ames test (*Salmonella* revertant test). BaP was evaluated as Class 2A (probably carcinogenic to humans) in IARC classification [1], and has been recently upgraded to Class 1 (carcinogenic to humans) [2]. BaP is used as a marker for carcinogenic risk of PAHs in ambient air, and unit risk of PAHs expressed as BaP for carcinogenesis is estimated to be 9×10^{-2} per μg/m^3 inhaled air (based on human studies) by the WHO Regional Office for Europe [3]. Unit risk of BaP in drinking water is also estimated to be 2.1×10^{-4} per μg/L drinking water (based on animal experiments) by the United States Environmental Protection Agency [4]. Thus, a concentration of BaP of 0.1 ng/m^3 in air and 50 ng/L in drinking water provides a cancer risk of 10^{-5} (1 in 100,000). If the daily intake of air and drinking water is set at 15 m^3 and 2 L, respectively, according to the standard default values for adults, the daily intake of BaP for a cancer risk level of 10^{-5} is estimated to be 1.5 ng for inhaled air and 100 ng for drinking water. These estimations suggest that exposure via air is a more sensitive pathway for the induction of cancer by BaP than exposure via drinking water. The target value for BaP in ambient air is 1 ng/m^3 in the EU [5], and the air quality standard for BaP as an annual average is 0.25 ng/m^3 in the UK; this value is derived from the lowest exposure level for the occurrence of lung cancer by occupational inhalation [6].

BaP has been detected in ambient air in association with SPM in many countries, especially in urban and industrial areas, and the concentrations of individual PAHs in the air range from <0.1 to 100 ng/m^3 [7]. In Japan, a report by the Ministry of the Environment documents the air concentrations of BaP at monitoring stations (366 points in 2007) in urban areas as part of a systematic nationwide monitoring managed by the Ministry and local government. The average concentration of BaP was 0.78 ng/m^3 (range, 0.05–8.1 ng/m^3) in 1998, but gradually decreased to 0.26 ng/m^3 (0.00038–1.8 ng/m^3) in 2007 [8].

In addition to BaP, various mutagenic and carcinogenic PAHs and nitro-PAHs are also released into the environment, especially in urban areas, as combustion products associated with diesel exhaust particles (DEP) and SPM. Several PAHs—including BaP, benzo[b]fluoranthene, benzo[j]fluoranthene, benzo[k]fluoranthene, chrysene, dibenzo[a,h] anthracene, and indeno[1,2,3,-cd]pyrene—were identified as carcinogens in intralung application experiments in rats [6]. For example, dibenzo[a,h]anthracene was shown to be 2.54 times more carcinogenic than BaP [6]. Among the nitro-PAHs, the dinitropyrene (DNP) isomers have been well tested for mutagenicity and carcinogenicity. For example, 1,3-, 1,6-,

and 1,8-DNP show higher mutagenic activity than BaP as determined by the Ames test [9], and intratracheal administration of 1,6-DNP induced lung tumors in hamsters [10] and rats [11]. The mutagenic activity of BaP requires cytochrome P450-mediated metabolic activation, whereas DNPs are mutagenic without metabolic activation [9], thus suggesting that BaP and DNPs have different modes of mutagenicity. Investigations of the *in vivo* mutagenicity of BaP and 1,6-DNP by intratracheal administration in transgenic *gpt* delta mice (a transgenic mouse model for detecting mutations; see section 3) show that the *in vivo* mutagenicity of 1,6-DNP [12] was about 20 times higher than that of BaP [13]. The concentration of 1,6-DNP in DEP is estimated to be about one-tenth that of BaP [14], indicating that the mutagenic potency of 1,6-DNP in DEP (*in vivo* mutagenicity × concentration) may be comparable to that of BaP. Apart from the DNP isomers, several nitro-PAH compounds, e.g., nitro-benzanthrone and nitro-benzopyrene, are mutagenic and carcinogenic. The intratracheal administration of 3-nitrobenzanthrone (3NBA) produces DNA adducts [15] and induces tumors in rat lungs [16]. 3,6-Dinitrobenzo[e]pyrene, which was originally detected in soil in Japan, shows potent mutagenic activity *in vitro* that is comparable to those estimated for 1,6- and 1,8-DNP [17, 18].

2. DNA Adduct Formation in the Lung of Experimental Animals by *In Situ* Exposure to Urban Air

PAHs and nitro-PAHs incorporated into lung, liver, and other target organs become genotoxic when converted to reactive electrophilic metabolites, known as reactive intermediates, by cytochrome P450 (CYP)-mediated monooxygenation. BaP is oxidized to BaP diol-epoxide (BPDE) by inducible CYP1A1 and CYP1A2 [19]. These reactive intermediates covalently bind genomic DNA, mainly on guanine, resulting in the formation of DNA adducts [20]. DNA repair systems can remove adducts, but adducts that are not removed can induce mismatching of DNA base pairs during DNA replication and thus cause gene mutations [21]. BaP, which forms BPDE-DNA adducts with guanine, induces G:C to T:A transversions *in vivo* [13, 22]. Mutations induced in cell growth or cell cycle genes can transform a normal somatic cell into a cancer cell, thus initiating tumor formation.

DNA adduct formation induced by environmental pollutants is a key event in mutagenesis and carcinogenesis. A simple test of the genotoxicity of air pollutants is to assess the formation of DNA adducts in the lungs of experimental animals exposed on site to polluted air ('*in situ* exposure'). In one such study, from 1995 to 1996, Wistar rats were maintained in a small-animal housing facility beside a main highway intersection in the Tokyo metropolitan area, and were exposed to the ambient air for up to 60 weeks; control rats were exposed to HEPA/charcoal-filtered ambient air [23]. The average monthly concentration of SPM < 2 μm was 51.8 μg/m^3 (range, 29.1–78.8 μg/m^3), whereas that for SPM < 11 μm was 76.5 μg/m^3 (50.4–108.3 μg/m^3). This experiment was originally designed for evaluating the effects of urban air on the respiratory system. After exposure to the ambient air, DNA adducts were analyzed by the ^{32}P-postlabeling assay, which involves nuclease P1 treatment and the separation of ^{32}P-postlabeled nucleotides by thin-layer

chromatography [24]. The level of DNA adduct formation was defined as the relative adduct level (RAL) which was determined by calculating the level of radioactivity in the adduct nucleotides per (radioactivity in total nucleotides × dilution factor). After 4 weeks' exposure to the urban air, the RAL of total DNA adducts in the lung and of the major DNA adduct in the liver increased from control levels of $0.8/10^8$ and $1.3/10^8$ nucleotides to $13.1/10^8$ and $6.6/10^8$ nucleotides, respectively [23]. However, the RAL in the lung decreased to a steady level of around $3/10^8$ nucleotides after prolonged exposure for over 12 weeks. This decrease was also observed in the liver, thus suggesting that prolonged exposure to air pollution activates the DNA repair system.

After *in situ* exposure of rats for 24 h to coke oven emissions, which contain carcinogenic PAHs and BaP at 892 and 118 ng/m^3, respectively, DNA adduct formation was induced in the lung and in extrapulmonary tissues [25]. The RAL of total DNA adducts was about $4.8/10^8$ nucleotides in both the liver and lung, but was lower at about $0.8/10^8$ nucleotides in white blood cells (WBCs). By comparison, the RAL of the BaP–DNA adduct, the major DNA adduct induced, was elevated to $1.6/10^8$ nucleotides in the lung, $1.3/10^8$ in the heart, and $0.5/10^8$ in WBCs compared with control rats ($0.3/10^8$ nucleotides in the lung, $0.2/10^8$ in the liver, and $0.2/10^8$ in WBCs). DNA adduct formation in rat liver and kidney was also observed after a single intratracheal administration of 3NBA [15]. Pollutants, such as PAHs and nitro-PAHs, absorbed into the lung have been shown to be systemically transported from the lung to other organs [15, 23, 25], but the mechanism underlying their movement to other organs remains unknown.

An *in situ* exposure study to estimate the mutagenicity of urban air was conducted in Hamilton Harbor, Ontario, Canada [26]. In this study, mice were housed near steel mills and a major highway, and were exposed *in situ* to ambient air containing a mean of 93.8 μg/m^3 total suspended particles and 8.3 ng/m^3 PAHs [26]. The RAL of DNA adducts in the lung was significantly higher after 3 weeks' exposure ($1/10^8$ nucleotides) compared with control mice breathing HEPA-filtered air ($0.7/10^8$ nucleotides). Prolonged exposure to the ambient air for 10 weeks, followed by maintenance of animals in the laboratory for 6 weeks, induced 1.58-fold increase in sperm mutation frequency of expanded simple tandem repeat compared with the control mice.

Observations by *in situ* exposure studies suggest that mutagenic compounds, such as PAHs and nitro-PAHs, in SPM in urban air can produce DNA adducts that cause gene mutations.

3. DNA Adduct Formation and *In Vivo* Mutagenesis by Exposure to Diesel Exhaust

Methods for detecting the genotoxicity of xenobiotics in somatic cells include the micronuclear test and the chromosomal aberration assay [27]. A comprehensive method for assessing mutations in somatic cells and germ cells is the transgenic rodent mutation assay, which can detect and quantify mutations, including base substitutions, deletions, and insertions [28]. In the assay, multiple copies of a target gene (*E. coli* gene) carried on a shuttle vector are integrated into genomic DNA. Four types of transgenic rodent models have

been developed: the Muta mouse, the Big Blue mouse and rat, the *gpt* delta mouse and rat, and the *rpsL* gene transgenic mouse model. In the Muta mouse, the *lacZ* gene, encoding beta-galactosidase, on a lambda phage is integrated into the genomic DNA. The Big Blue mouse and rat are based on the integration into the genome of the *lacI* (*lac* operon repressor) gene on a lambda phage. Transgenic medaka fish (*Oryzias latipes*) have also been generated with *lacI* gene on a lambda phage for monitoring of mutagens in aquatic environment [29]. The *gpt* delta transgenic mouse and rat [30] have the *gpt* gene, encoding guanine phosphoribosyl transferase, integrated into the genome. In this model, large DNA deletions are detectable using the *red/gam* gene located on the lambda phage [31]. In the *rpsL* gene transgenic mouse model, *rpsL*, which confers streptomycin sensitivity in *E. coli*, is the mutational target gene and is integrated into the mouse genome on a plasmid [32]. Transgenic zebrafish harboring *rpsL* have also been generated for mutation studies [33]. The target genes that have integrated into the genomic DNA of the transgenic model animals are rescued to *E. coli* by transfection; the mutated target gene is then detected by positive selection (or negative selection for *lacZ* mutation assay) of transfected *E. coli*. Mutant frequency (MF) is defined as number of mutant colonies or plaques per titer. Sequence analysis of mutated target genes can detect and quantify the types of mutations.

To assess the DNA adduct-producing potency of SPM and its relationship to *in vivo* mutagenicity, Big Blue rats were exposed to diesel engine exhaust (DE), a major source of SPM in urban areas and a model air pollutant [14]. After continuous inhalation by the rats of DE at either 1 or 6 mg SPM/m^3 for 4 weeks, the RAL of DNA adducts was $23/10^8$ and $48/10^8$ nucleotides, respectively. The inhalation of 6 mg SPM/m^3 DE gave a significant ($P<0.01$) elevation of MF: 4.25×10^{-5} in lung exposed to DE compared with 0.88×10^{-5} in control lung. By comparison, inhalation of 1 mg SPM/m^3 did not cause a significant increase in MF. Although the concentration of SPM in DE at 6 mg/m^3 is over 78 times the concentration (76.5 μg/m^3) found in urban air, some of which may originate from DE, the DNA adduct level induced by DE inhalation was only 3.7 times higher than that induced by urban air ($13.1/10^8$) over the same period (4 weeks) of exposure [23]. This observation may be explained by a non-linear (saturated) dose response between the level of exposure and DNA adduct at high dose, which was demonstrated in rat lung exposed to a coal-tar pitch aerosol [34].

Increase in MF by inhalation of DE was also shown in the lung of *gpt* delta mice [35]. After continuous inhalation of DE at 3 mg SPM/m^3 for 4 weeks, the MF in the lung elevated to significantly higher levels (1.06×10^{-5}) than in the control lung (0.61×10^{-5}) ($P<0.05$). The DNA adduct level was not determined in the lungs of *gpt* delta mice exposed to DE, but was determined in a separate experiment under the same conditions of DE exposure: the RAL of DNA adducts increased to $11/10^8$ nucleotides ($3/10^8$ nucleotides in the control) [36]. By comparison, a higher concentration of DE (20 mg SPM/m^3) and a shorter exposure period (a single 90-min exposure period on each of four consecutive days) resulted in a slight but significant increase in DNA adduct formation in the lung of the Muta mouse 1 h after the last exposure period [37]. Under these conditions, the MF in the lung was not elevated [37].

The mutagenic and DNA adduct-forming potencies of PAH and nitro-PAH in the lung were examined by a single intratracheal administration. Intratracheal administration of 10 mg BaP/animal (30–40 mg/body weight) in Big Blue rats induced a doubling in the MF from the

control level of 3.1×10^{-5} to 6.1×10^{-5} at 4 weeks after dosing [38], while the RAL in BaP-treated lungs was $5.1/10^8$ nucleotides. BaP administration induced a lower RAL in the lung than did DE inhalation, but the increase in MF was similar in both treatments [14,38]. Intratracheal administration of 1 mg BaP (about 40 mg/body weight) increased the MF in *gpt* delta mouse lungs to 2.52×10^{-5} from the control MF of 0.60×10^{-5} [13]. The mutagenic potency of BaP in lungs is similar in rats and mice when the BaP dose is normalized to body weight. In the lungs of *gpt* delta mice, 1,6-DNP gave a markedly higher MF of 31×10^{-5} per mg [12] than that of BaP at 1.7×10^{-5} per mg [13]. The type of mutations induced by DE, BaP, and 1,6-DNP were assessed. The G:C→A:T transition was the major base substitution induced by DE in the lungs of Big Blue rats [14] and *gpt* delta mice [35]. By comparison, BaP and 1,6-DNP tended to induce G:C→T:A transversions and G:C→A:T transitions, respectively [12, 13]. Interestingly, the mutation hot spots induced by DE inhalation were similar to those induced by 1,6-DNP (Fig. 1), but these sites were different from those induced by BaP [13]. These results suggest that DNPs and related compounds are the major mutagens in DE.

In the transgenic rodent study, the RAL for DNA adducts of $>5/10^8$ nucleotides, which was produced by intratracheal administration of BaP [38], possibly gave a markedly increase in the MF in the lung. Exposure of V79 cells to the BaP metabolite BPDE revealed that the MF of the *HPRT* gene and the RAL for DNA adducts gave a concentration-dependent linear increase with an MF-to-RAL ratio of 4.39×10^{-9} [39]. However, it was unclear how the levels of DNA adduct formation (RAL) induced by the mutagen were quantitatively related to *in vivo* mutagenicity.

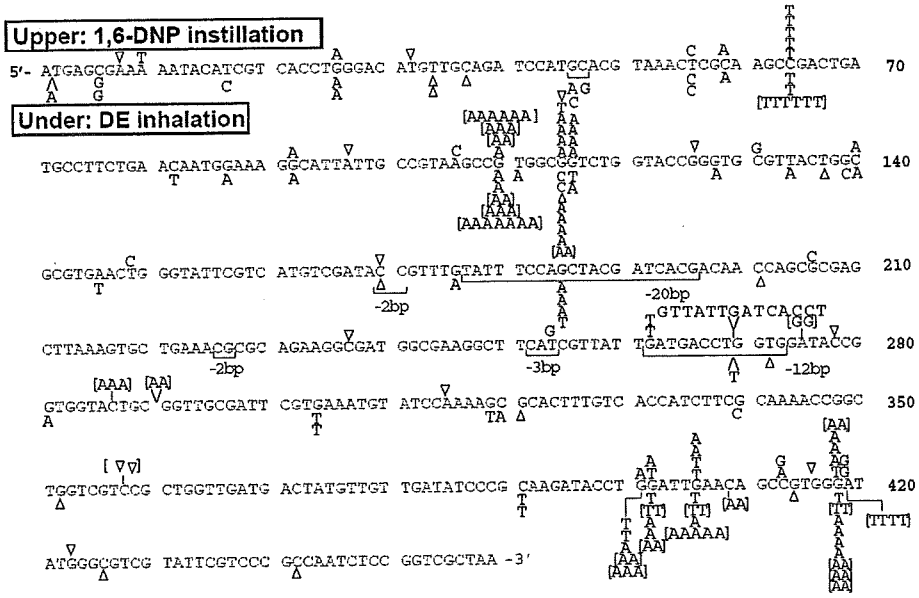

Figure 1. Overall distribution of the mutations detected in the *gpt* gene in the lungs of mice treated with 1,6-DNP by intratracheal administration and those treated with DE by inhalation exposure. The mutations induced by 1,6-DNP [12] and DE [35] are shown, respectively, above and below the *gpt* sequence. The number of characters in parentheses is the number of mutations in one mouse. Δ, one base deletion; half-boxes, deleted nucleotides; V, a position of insertion.

4. DNA Adduct Formation in Humans

DNA adducts are useful biomarkers for monitoring exposure to PAHs and may be useful for assessing the potential mutagenicity of environmental pollutants. Blood cells are appropriate for detecting DNA adducts induced as a consequence of PAH exposure, and have been used in epidemiological studies in Poland, Italy, Denmark, Greece, several other European countries, and Thailand [40]. These studies revealed that the level of DNA adduct formation is higher in areas exposed to more PAHs than in areas exposed to less PAHs. Since blood cells are rapidly turned over, analysis of DNA adduct formation in human lung autopic samples have been tried, despite sampling difficulties, for monitoring long-term exposure to PAHs in ambient air. The ^{32}P-postlabeling assay showed that the total RAL for smokers was 1.5–34.3/10^8 nucleotides, whereas that for non-smokers was 1.9–3.3/10^8 nucleotides [41]. Lewtas et al. revealed that the average RAL in autopic samples was 9.42 (range, 8.34–11.1)/10^8 nucleotides in smokers and 3.15 (1.49–4.80)/10^8 nucleotides in nonsmokers [42]. The RALs for DNA adducts were also analyzed in biopsy samples of bronchial tissue and were found to be 3.45 ± 1.62/10^8 in nonsmokers, 3.93 ± 1.92/10^8 in former smokers, and 5.53 ± 2.13/10^8 in smokers [43]. In a study in Florence, Italy, the level of BPDE–DNA adducts was measured by high-performance liquid chromatography / synchronous fluorescence in autopic samples from individuals exposed to air in which PAHs were monitored [44]. The average level of total adducts was 1.76 ± 1.69/10^8 nucleotides in nonsmokers, 4.04 ± 2.37/10^8 nucleotides in ex-smokers, and 4.46 ± 5.76/10^8 nucleotides in smokers. Furthermore, the total BPDE–DNA adduct level correlated positively with the BaP level in the lung. In this study, the level of PAHs in air was 15–35 ng/m^3. In the Florence area, analysis of the relationship between the DNA adduct level in leukocytes and exposure to SPM < 10 μm in diameter (PM_{10}) revealed that the DNA adduct levels in nonsmoking workers reflected the level of PM_{10} exposure in high traffic urban area from 1993 to 1998 [45].

5. Conclusion

As described in Section 4, the level of DNA adducts in the lungs of nonsmokers was estimated to be 1.9–3.3/10^8 nucleotides [41], which is lower than the maximum level in the lungs of rats exposed to urban air, but marginal to the steady level (around 3/10^8 nucleotides). These results demonstrate that inhalation by experimental animals can accurately reflect the impact of air pollutants in human lungs, and thus provides a useful tool for monitoring the total impact of air pollutants (e.g., DNA adduct formation by PAHs in the air). Recently, *in vivo* mutation data has been analyzed for informing the cancer risk assessment process [46]. However, further studies are required for evaluating the relationship between the DNA adduct level and *in vivo* mutagenicity by *in situ* exposure to urban air or a model pollutant, and the relationship between the *in vivo* mutagenicity and carcinogenicity for quantitative health risk assessments, especially for the risk of lung cancer from air pollution.

Acknowledgments

We thank Drs. T. Nohmi and K. Masumura (National Institute for Health Sciences, Japan) for their collaboration in a *gpt* delta mouse study, and Dr. K. Amanuma (NIES; present address, NIHS) for her helpful suggestions and discussion.

References

[1] International Agency for Research on Cancer. (1983) Benzo[a]pyrene. *Monogr Eval Carcinog Risk Chem Hum. 32*, 211-224.

[2] International Agency for Research on Cancer. Air Pollution, Part 1, Some Non-heterocyclic Polycyclic Aromatic Hydrocarbons and Some Related Industrial Exposures. *Monogr Eval Carcinog Risk Chem Hum. 92* in preparation. (http://monographs.iarc.fr/ENG/Classification/crthgr01.php)

[3] World Health Organization Regional Office for Europe. Air Quality Guidelines for Europe, 2nd ed.. WHO Regional Publications, European Series, No. 91. Copenhagen: World Health Organization; 2000.

[4] Integrated Risk Information System. http://www.epa.gov/NCEA/iris/subst/0136.htm. United States Environmental Protection Agency.

[5] DIRECTIVE 2004/107/EC OF THE EUROPEAN PARLIAMENT AND OF THE COUNCIL of 15 December 2004 relating to arsenic, cadmium, mercury, nickel and polycyclic aromatic hydrocarbons in ambient air. 26.1.2005, L23/3-16.

[6] Pufulete M, Battershill J, Boobis A, & Fielder R. (2004) Approaches to carcinogenic risk assessment for polycyclic aromatic hydrocarbons: a UK perspective. *Regul Toxicol Pharmacol. 40*, 54-66.

[7] World Health Organization. Environmental Health Criteria 202; Selected Non-heterocyclic Polycyclic Aromatic Hydrocarbons. Geneva: International Programme on Chemical Safety; 1998.

[8] The Ministry of the Environment, Japan. http://www.env.go.jp/air/osen/monitoring/mon_h19/tab9.html (in Japanese)

[9] World Health Organization. Environmental Health Criteria 229; Selected Nitro- and Nitro-oxy-polycyclic Aromatic Hydrocarbons. Geneva: International Programme on Chemical Safety; 2003.

[10] Takayama S, Ishikawa T, Nakajima H, & Sato S. (1985) Lung carcinoma induction in Syrian golden hamsters by intratracheal instillation of 1,6-dinitropyrene. *Jpn J Cancer Res. 76*, 457-461.

[11] Iwagawa M, Maeda T, Izumi K, Otsuka H, Nishifuji K, Ohnishi & Y, Aoki S. (1989) Comparative dose-response study on the pulmonary carcinogenicity of 1,6-dinitropyrene and benzo[a]pyrene in F344 rats. *Carcinogenesis. 10*, 1285-1290.

[12] Hashimoto AH, Amanuma K, Hiyoshi K, Takano H, Masumura K, Nohmi T, & Aoki. Y. (2006) In vivo mutagenesis in the lungs of gpt-delta transgenic mice treated intratracheally with 1,6-dinitropyrene. *Environ Mol Mutagen. 47*, 277-283.

[13] Hashimoto AH, Amanuma K, Hiyoshi K, Takano H, Masumura K, Nohmi T, & Aoki Y. (2005) In vivo mutagenesis induced by benzo[a]pyrene instilled into the lung of gpt delta transgenic mice. *Environ Mol Mutagen. 45*, 365-373.

[14] Sato H, Sone H, Sagai M, Suzuki KT, & Aoki Y. (2000) Increase in mutation frequency in lung of Big Blue rat by exposure to diesel exhaust. *Carcinogenesis. 21*, 653-661.

[15] Arlt VM. (2005) 3-Nitrobenzanthrone, a potential human cancer hazard in diesel exhaust and urban air pollution: a review of the evidence. *Mutagenesis. 20,* 399-410.

[16] Nagy E, Zeisig M, Kawamura K, Hisamatsu Y, Sugeta A, Adachi S, & Möller L. (2005) DNA adduct and tumor formations in rats after intratracheal administration of the urban air pollutant 3-nitrobenzanthrone. *Carcinogenesis. 26*, 1821-1828.

[17] Watanabe T, Hasei T, Takahashi T, Asanoma M, Murahashi T, Hirayama T, & Wakabayashi K. (2005) Detection of a novel mutagen, 3,6-dinitrobenzo[e]pyrene, as a major contaminant in surface soil in Osaka and Aichi Prefectures, Japan. *Chem Res Toxicol. 18,* 283-289.

[18] Watanabe T, Takahashi K, Konishi E, Hoshino Y, Hasei T, Asanoma M, Hirayama T, & Wakabayashi K. (2008) Mutagenicity of surface soil from residential areas in Kyoto city, Japan, and identification of major mutagens. *Mutat Res. 649*, 201-212.

[19] Nebert DW, & Negishi M. (1982) Multiple forms of cytochrome P-450 and the importance of molecular biology and evolution. *Biochem Pharmacol. 31*, 2311-2317.

[20] Miller EC, & Miller JA. (1981) Mechanisms of chemical carcinogenesis. *Cancer. 47(5 Suppl)*, 1055-1064.

[21] Harris CC. (1985) Future directions in the use of DNA adducts as internal dosimeters for monitoring human exposure to environmental mutagens and carcinogens. *Environ Health Perspect. 62*, 185-91.

[22] Bailleul B, Brown K, Ramsden M, Akhurst RJ, Fee F, & Balmain A. (1989) Chemical induction of oncogene mutations and growth factor activity in mouse skin carcinogenesis. *Environ Health Perspect. 81*, 23-27.

[23] Sato H, Suzuki KT, Sone H, Yamano Y, Kagawa J, & Aoki Y. (2003) DNA-adduct formation in lungs, nasal mucosa, and livers of rats exposed to urban roadside air in Kawasaki City, Japan. *Environ Res. 93*, 36-44.

[24] Reddy MV, & Randerath K. (1986) Nuclease P1-mediated enhancement of sensitivity of 32P-postlabeling test for structurally diverse DNA adducts. *Carcinogenesis. 7*, 1543-51.

[25] Binková B, Dobiás L, Wolff T, & Srám RJ. (1994) 32P-postlabeling analysis of DNA adducts in tissues of rats exposed to coke-oven emissions. *Mutat Res. 307*, 355-63.

[26] Yauk C, Polyzos A, Rowan-Carroll A, Somers CM, Godschalk RW, Van Schooten FJ, Berndt ML, Pogribny IP, Koturbash I, Williams A, Douglas GR, & Kovalchuk O. (2008) Germ-line mutations, DNA damage, and global hypermethylation in mice exposed to particulate air pollution in an urban/industrial location. *Proc Natl Acad Sci USA. 105*, 605-10.

[27] World Health Organization. Environmental Health Criteria 51; Guide to Short-term Tests for Detecting Mutagenic and Carcinogenic Chemicals. Geneva: International Programme on Chemical Safety; 2003.

[28] Lambert IB, Singer TM, Boucher SE, & Douglas GR. (2005) Detailed review of transgenic rodent mutation assays. *Mutat Res. 590*, 1-280.

[29] Winn RN, Norris MB, Brayer KJ, Torres C, & Muller SL. (2000) Detection of mutations in transgenic fish carrying a bacteriophage lambda cII transgene target. *Proc Natl Acad Sci USA. 97*, 12655-12660.

[30] Hayashi H, Kondo H, Masumura K, Shindo Y, & Nohmi T. (2003) Novel transgenic rat for in vivo genotoxicity assays using 6-thioguanine and Spi- selection. *Environ Mol Mutagen. 41*, 253-259.

[31] Nohmi T, Katoh M, Suzuki H, Matsui M, Yamada M, Watanabe M, Suzuki M, Horiya N, Ueda O, Shibuya T, Ikeda H, & Sofuni T. (1996) A new transgenic mouse mutagenesis test system using Spi- and 6-thioguanine selections. *Environ Mol Mutagen. 28*, 465-470.

[32] Gondo Y, Shioyama Y, Nakao K, & Katsuki M. (1996) A novel positive detection system of in vivo mutations in rpsL (strA) transgenic mice. *Mutat Res. 360*, 1-14.

[33] Amanuma K, Takeda H, Amanuma H, & Aoki Y. (2000) Transgenic zebrafish for detecting mutations caused by compounds in aquatic environments. *Nat Biotechnol. 18*, 62-65.

[34] Lewtas J, Walsh D, Williams R, & Dobiás L. (1997) Air pollution exposure-DNA adduct dosimetry in humans and rodents: evidence for non-linearity at high doses. *Mutat Res. 378*, 51-63.

[35] Hashimoto AH, Amanuma K, Hiyoshi K, Sugawara Y, Goto S, Yanagisawa R, Takano H, Masumura K, Nohmi T, & Aoki Y. (2007) Mutations in the lungs of gpt delta transgenic mice following inhalation of diesel exhaust. *Environ Mol Mutagen. 48*, 682-693.

[36] Aoki Y, Sato H, Nishimura N, Takahashi S, Itoh K, & Yamamoto M. (2001) Accelerated DNA adduct formation in the lung of the Nrf2 knockout mouse exposed to diesel exhaust. *Toxicol Appl Pharmacol. 173*, 154-160.

[37] Dybdahl M, Risom L, Bornholdt J, Autrup H, Loft S, & Wallin H. (2004) Inflammatory and genotoxic effects of diesel particles in vitro and in vivo. *Mutat Res. 562*, 119-131.

[38] Loli P, Topinka J, Georgiadis P, Dusinská M, Hurbánková M, Kovácikóvá Z, Volkovová K, Wolff T, Oesterle D, & Kyrtopoulos SA. (2004) Benzo[a]pyrene-enhanced mutagenesis by asbestos in the lung of lambda-lacI transgenic rats. *Mutat Res. 553*, 79-90.

[39] Helleberg H, Xu H, Ehrenberg L, Hemminki K, Rannug U, & Törnqvist M. (2001) Studies of dose distribution, premutagenic events and mutation frequencies for benzo[a]pyrene aiming at low dose cancer risk estimation. *Mutagenesis. 16*, 333-337.

[40] Vineis P, & Husgafvel-Pursiainen K. (2005) Air pollution and cancer: biomarker studies in human populations. *Carcinogenesis. 26*, 1846-1855.

[41] Phillips DH, Hewer A, Martin CN, Garner RC, & King MM. (1988) Correlation of DNA adduct levels in human lung with cigarette smoking. *Nature. 336*, 790-792.

[42] Lewtas J, Mumford J, Everson RB, Hulka B, Wilcosky T, Kozumbo W, Thompson C, George M, Dobiás L, Srám R, Xueming L, & Gallagher J. (1993) Comparison of DNA adducts from exposure to complex mixtures in various human tissues and experimental systems. *Environ Health Perspect. 99*, 89-97.

[43] Phillips DH, Schoket B, Hewer A, Bailey E, Kostic S, & Vincze I. (1990) Influence of cigarette smoking on the levels of DNA adducts in human bronchial epithelium and white blood cells. *Int J Cancer. 46*, 569-575.

[44] Lodovici M, Akpan V, Giovannini L, Migliani F, & Dolara P. (1998) Benzo[a]pyrene diol-epoxide DNA adducts and levels of polycyclic aromatic hydrocarbons in autoptic samples from human lungs. *Chem Biol Interact. 116*, 199-212.

[45] Palli D, Saieva C, Munnia A, Peluso M, Grechi D, Zanna I, Caini S, Decarli A, Sera F, & Masala G. (2008) DNA adducts and PM10 exposure in traffic-exposed workers and urban residents from the EPIC-Florence City study. *Sci Total Environ. 403*, 105-112.

[46] Moore MM, Heflich RH, Haber LT, Allen BC, Shipp AM, & Kodell RL. (2008) Analysis of in vivo mutation data can inform cancer risk assessment. *Regul Toxicol Pharmacol. 51*, 151-161.

Oncogene (2009) 28, 1142–1150

www.nature.com/onc

ORIGINAL ARTICLE

A novel protein, MAPO1, that functions in apoptosis triggered by O^6-methylguanine mispair in DNA

K Komori[1], Y Takagi[2], M Sanada[3], T-H Lim[4], Y Nakatsu[4], T Tsuzuki[4], M Sekiguchi[1,2] and M Hidaka[1,3,4]

[1]*Department of Molecular Biology, Biomolecular Engineering Research Institute, Suita, Japan;* [2]*Frontier Research Center, Fukuoka Dental College, Fukuoka, Japan;* [3]*Department of Physiological Science and Molecular Biology, Fukuoka Dental College, Fukuoka, Japan and* [4]*Department of Medical Biophysics and Radiation Biology, Faculty of Medical Sciences, Kyushu University, Fukuoka, Japan*

O^6-Methylguanine produced in DNA induces mutation due to its ambiguous base-pairing properties during DNA replication. To suppress such an outcome, organisms possess a mechanism to eliminate cells carrying O^6-methylguanine by inducing apoptosis that requires the function of mismatch repair proteins. To identify other factors involved in this apoptotic process, we performed retrovirus-mediated gene-trap mutagenesis and isolated a mutant that acquired resistance to a simple alkylating agent, *N*-methyl-*N*-nitrosourea (MNU). However, it was still sensitive to methyl methanesulfonate, 1-(4-amino-2-methyl-5-pyrimidinyl)methyl-3-(2-chloroethyl)-3-nitrosourea, etoposide and ultraviolet irradiation. Moreover, the mutant exhibited an increased mutant frequency after exposure to MNU. The gene responsible was identified and designated *Mapo1* (O^6-methylguanine-induced apoptosis 1). When the expression of the gene was inhibited by small interfering RNA, MNU-induced apoptosis was significantly suppressed. In the *Mapo1*-defective mutant cells treated with MNU, the mitochondrial membrane depolarization and caspase-3 activation were severely suppressed, although phosphorylation of p53, CHK1 and histone H2AX was observed. The orthologs of the *Mapo1* gene are present in various organisms from nematode to humans. Both mouse and human MAPO1 proteins expressed in cells localize in the cytoplasm. We therefore propose that MAPO1 may play a role in the signal-transduction pathway of apoptosis induced by O^6-methylguanine-mispaired lesions.
Oncogene (2009) **28,** 1142–1150; doi:10.1038/onc.2008.462; published online 12 January 2009

Keywords: apoptosis; gene-trap mutagenesis; *Mapo1*; MGMT; O^6-methylguanine

Correspondence: Dr M Hidaka, Department of Physiological Science and Molecular Biology, Fukuoka Dental College, 2-15-1 Tamura, Sawara-ku, Fukuoka 814-0193, Japan.
E-mail: hidaka@college.fdcnet.ac.jp
Received 10 June 2008; revised 17 November 2008; accepted 21 November 2008; published online 12 January 2009

Introduction

The modification of DNA bases occurs spontaneously during normal cell growth, and the rate of formation of modified bases increases considerably when cells are exposed to radiation and certain chemical agents. O^6-methylguanine is one of such bases produced by the action of simple alkylating agents, such as *N*-methyl-*N*-nitrosourea (MNU) and *N*-methyl-*N'*-nitro-*N*-nitrosoguanidine (Beranek, 1990). This modified base can pair with thymine as well as cytosine during DNA replication, and a G:C to A:T transition mutation ensues after two cycles of DNA replication (Coulondre and Miller, 1977; Loechler *et al.*, 1984; Ito *et al.*, 1994). To prevent such outcomes, organisms possess a specific DNA repair enzyme, O^6-methylguanine-DNA methyltransferase (MGMT), which transfers a methyl group from the O^6-methylguanine moiety to its own molecule, thereby repairing the DNA lesion in a single-step reaction (Pegg, 2000; Margison and Santibanez-Koref, 2002; Kaina *et al.*, 2007). *Mgmt*$^{-/-}$ mice, which are defective in the methyltransferase gene, are hypersensitive to the killing effect of alkylating agents and suffer from severe damage in the bone marrow and intestinal mucosa, which are largely composed of rapidly growing cells (Tsuzuki *et al.*, 1996; Sakumi *et al.*, 1997; Glassner *et al.*, 1999). Studies with cell lines derived from *Mgmt*$^{-/-}$ mice further revealed that O^6-methylguanine-induced cell death occurs by apoptosis, which requires at least one round of DNA replication for its induction (Tominaga *et al.*, 1997; Meikrantz *et al.*, 1998).

A notable feature of O^6-methylguanine-induced apoptosis is the requirement of mismatch repair (MMR) proteins, such as MSH2 and MLH1 (Hickman and Samson, 1999; Pepponi *et al.*, 2003). Studies with cell lines derived from human tumors revealed that the lack of some of these gene functions rendered MGMT-deficient cells resistant to alkylating agents (Branch *et al.*, 1993; Kat *et al.*, 1993). Recent studies with *Mgmt*$^{-/-}$ *Mlh1*$^{-/-}$ cells, derived from gene-targeted mice, have shown that the MLH1 protein is indeed required for the execution of apoptosis triggered by O^6-methylguanine (Kawate *et al.*, 1998; Takagi *et al.*, 2003). We have shown that MutSα, consisting of MSH2 and

MSH6 proteins, and PCNA bind to O^6-methylguanine-containing DNA to form an initial complex, and MutLα, composed of MLH1 and PMS2, binds to this complex (Hidaka *et al.*, 2005). However, the precise mechanisms regarding how the MMR complex activates the apoptotic signal remain to be elucidated. Two hypotheses have so far been proposed: the MMR complex formed on chromatin might induce the apoptotic signal (Fishel, 1998) or abortive repair cycle initiated by the complex might lead to apoptosis (Karran, 2001).

The activation of ATR kinase and phosphorylation of its downstream targets have been shown to take place in an MMR protein-dependent manner in cells treated with MNU (Caporali *et al.*, 2004; Stojic *et al.*, 2004; Sanada *et al.*, 2007). The MMR protein-dependent release of cytochrome *c* from mitochondria and activation of caspases, which are hallmarks for apoptosis, also occur in the case of O^6-methylguanine-induced apoptosis (Ochs and Kaina, 2000; Takagi *et al.*, 2003; Hickman and Samson, 2004). As apoptosis caused by bulky DNA lesions that block DNA replication occurs even in cells deficient in MMR proteins (Peng *et al.*, 2007; Sanada *et al.*, 2007), the apoptosis pathway induced by O^6-methylguanine, which does not block DNA replication, appears to be distinct from the former. It is highly likely that other proteins are also involved in the pathway. Therefore, retrovirus-mediated gene-trap mutagenesis (Ishida and Leder, 1999; Wiles *et al.*, 2000; Guo *et al.*, 2004) was used to isolate a mutant, which exhibits an increased tolerance to a simple alkylating agent that produces O^6-methylguanine. The disrupted gene in the mutant was identified to be a novel gene, designated *Mapo1* (for O^6-methylguanine-induced apoptosis 1), which encodes a protein with a molecular mass of 125.6 kDa. Evidence is herein presented, which shows that the protein might be involved in the pathway of apoptosis induced by O^6-methylguanine adducts.

Results

Isolation of mutant cells defective in O^6-methylguanine-induced apoptosis

To perform insertional mutagenesis, we constructed a retrovirus-based gene-trap vector, pLHΔU3L, as illustrated in the upper part of Figure 1. The vector carries a promoterless hygromycin B resistance (Hyg^r) gene, together with a splice acceptor site and an internal ribosome entry site (IRES), which would facilitate efficient transcription and translation of the Hyg^r gene when integrated into any region, including an intron sequence, of actively transcribed genes. If the function of any gene indispensable for inducing apoptosis is lost by this insertional mutagenesis, we may expect that *Mgmt*-defective cells that are hypersensitive to a simple alkylating agent would become resistant to MNU. According to this experimental scheme (Figure 1), YT102 cells, a lung fibroblast cell line established from *Mgmt*-knockout mice (Takagi *et al.*, 2003), were infected

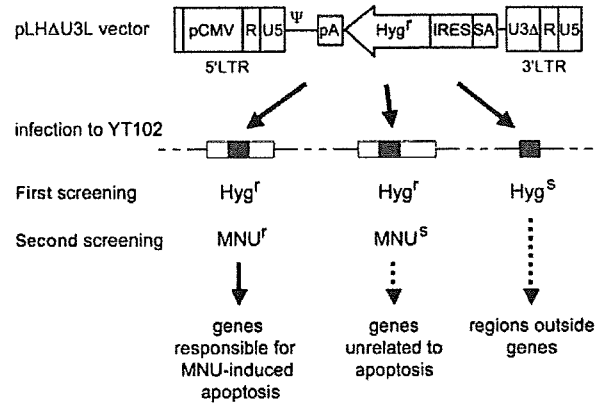

Figure 1 Retrovirus-mediated gene-trap mutagenesis. Schematic diagram of the pLHΔU3L vector is drawn at the top. ψ, packaging signal; Hyg^R, hygromycin-resistant gene; IRES, internal ribosome entry site; LTR, long terminal repeat; pA, poly A signal; pCMV, cytomegalovirus promoter; SA, splicing acceptor site. Flowchart of the mutant screening is shown at the bottom. A line represents the genomic DNA. White boxes on the line indicate genes, into which vector DNA drawn as gray boxes is integrated. Hyg^r, hygromycin resistant; Hyg^s, hygromycin sensitive; MNU^r, MNU resistant; MNU^s, MNU sensitive.

with the gene-trap vector pLHΔU3L and hygromycin-resistant (Hyg^r) cells were obtained. The population of Hyg^r cells carrying the vector sequence within actively transcribed genes was then subjected to selection with 0.4 mM MNU. The MNU-resistant (MNU^r) clones were isolated as candidates that have insertional mutations within the genes involved in MNU-induced apoptosis.

O^6-Methylguanine, which is a major cytotoxic adduct produced in DNA by treating the cells with low doses of MNU, can be repaired by a specific DNA repair enzyme, MGMT. As shown in Figure 2, YT102 cells are defective in this enzyme and readily undergo cell death after exposure to relatively low doses of MNU. In contrast, YT102M, a derivative of YT102 that stably expresses human MGMT (Figure 2a), is resistant to the treatment with such doses of MNU, indicating that the cell death induced in YT102 cells results from O^6-methylguanine. One of the isolated mutants exhibited a significantly high level of resistance to MNU, in comparison to the parental cell line YT102, without expressing MGMT. The expression levels of MMR proteins, namely MSH2, MSH6, MLH1 and PMS2, which are required for the recognition of the O^6-methylguanine-mispaired lesions, were not affected in the mutant (Figure 2a). We termed this clone KH101 and performed a survival assay with various doses of MNU. As calculated from the survival curves shown in Figure 2b, the doses required to give LD_{37} to KH101 and the parental *Mgmt*$^{-/-}$ strain, YT102, are 0.48 and 0.08 mM, respectively. Therefore, KH101 is approximately six times more resistant to MNU than the parental *Mgmt*$^{-/-}$ strain, due to inactivation of a certain gene that might be required for apoptosis. The level of resistance of KH101, however, is lower in comparison to YT103, which lacks both MGMT and MLH1 functions.

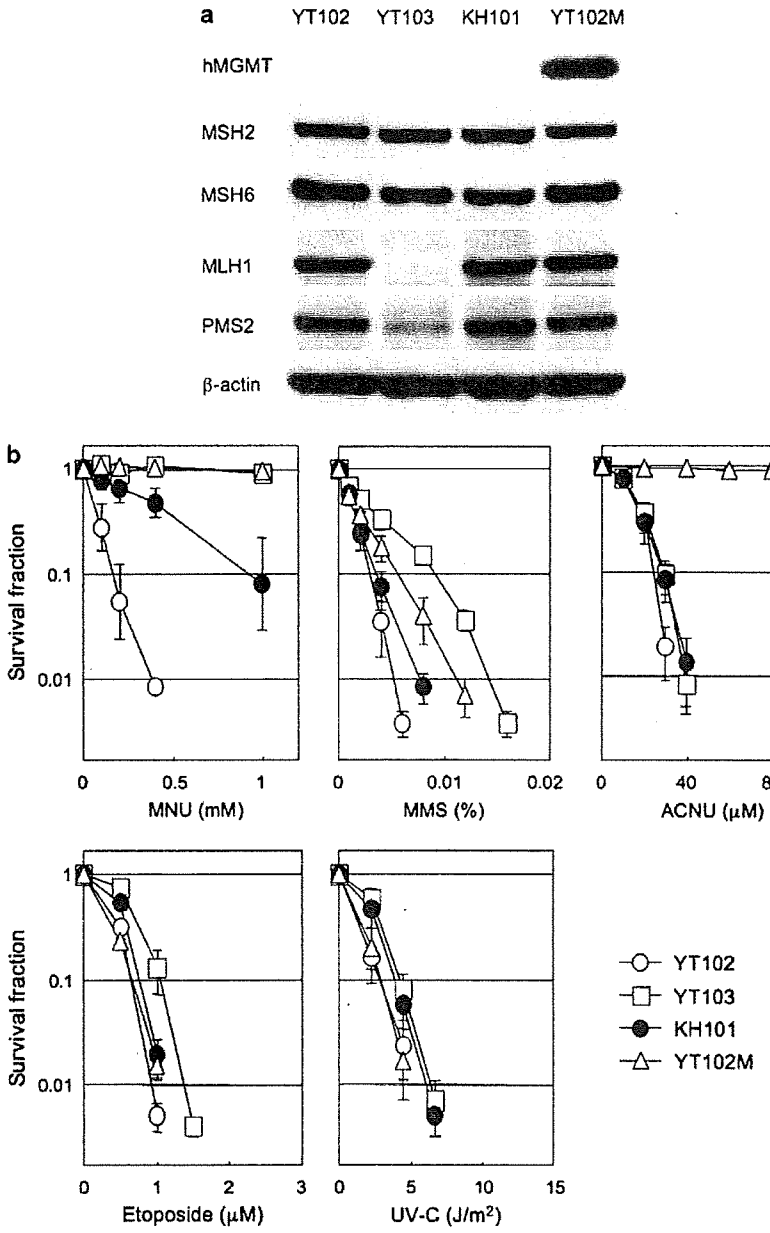

Figure 2 The sensitivities of various mutant cells to DNA-damaging agents. (a) The expression levels of O^6-methylguanine-DNA methyltransferase (MGMT) and mismatch repair (MMR) proteins in YT102, YT103, KH101 and YT102M cell lines. The MGMT and MMR proteins were detected with immunoblotting using specific antibodies. (b) The cells were treated with different concentrations of *N*-methyl-*N*-nitrosourea (MNU), methyl methanesulfonate (MMS) and 1-(4-amino-2-methyl-5-pyrimidinyl)methyl-3-(2-chloroethyl)-3-nitrosourea (ACNU) for 1 h, or etoposide for 12 h, and then were incubated in a drug-free medium for 6 days. For ultraviolet (UV) irradiation, the cells were exposed to different doses of UV-C. The numbers of colonies were counted and the survival fractions were determined. All experiments were performed three times and the standard deviations are shown in bars. Open circles, YT102 (*Mgmt*$^{-/-}$); open squares, YT103 (*Mgmt*$^{-/-}$ *Mlh1*$^{-/-}$); closed circles, KH101; open triangles, YT102M.

When treated with other DNA-damaging agents, methyl methanesulfonate (MMS), 1-(4-amino-2-methyl-5-pyrimidinyl)methyl-3-(2-chloroethyl)-3-nitrosourea (ACNU), etoposide and ultraviolet (UV)-C, which produce primarily N7-methylguanines and N3-methyladenines, DNA-interstrand crosslinks, DNA double-strand breaks and pyrimidine dimers, respectively, KH101 cells showed a similar degree of sensitivity to the parental strain YT102, although KH101 cells tended to be slightly more resistant than YT102 in all cases. YT103 and YT102M cells displayed increased resistance to MMS in comparison to YT102, as reported earlier (Kaina *et al.*, 1991; Glaab *et al.*, 1998). YT102 cells were quite resistant to ACNU as expected (Peng *et al.*, 2007;

Sanada *et al.*, 2007). These results imply that KH101 cells might have a defect in a gene involved in the induction of cell death caused by MNU-induced O^6-methylguanine.

MNU-induced mutant frequency

As O^6-methylguanine is a premutagenic DNA lesions, the mutation frequency would increase if cells carrying O^6-methylguanine are not eliminated by apoptosis (Takagi *et al.*, 2003). Therefore, we measured the mutant frequency of KH101 cells with respect to ouabain resistance, which can arise by a mutation in the Na^+/K^+ ATPase locus (Figure 3). As a control, we used YT102M, which is resistant to MNU, for its overexpression of the human MGMT protein. Without MNU treatment, YT102M and KH101 cells exhibited the same low level of mutant frequency, indicating that the defect in KH101 cells does not affect the spontaneous mutagenesis. The mutant frequencies of both strains increased on exposure to MNU, but the extent of increase in KH101 was far greater than that of YT102M. The level attained with KH101 cells was about six times higher than that of YT102M. This is consistent with the possibility that the gene product defective in KH101 cells may be involved in a process to execute apoptosis in cells carrying mutation-evoking DNA lesions.

Identification of the gene defective in KH101 mutant

To determine the genomic sequence into which the vector DNA has been integrated, we carried out inverse PCR using the genomic DNAs digested with several restriction enzymes as templates. The amplified DNA fragments, spanning the junctions between the genomic DNA and the integrated vector sequences, were cloned into a pGEM-Teasy plasmid, and the nucleotide sequences were determined. A database search revealed that the vector DNA to be integrated in a sequence corresponding to the first intron of a putative gene mKIAA1450 (GenBank accession no. XM_907047) (Figure 4a), located in the E3 locus of mouse chromosome 3. The prospective gene is composed of at least 18 exons and would encode a polypeptide comprising 1138 amino acids. The gene is novel, and thus, we named it *Mapo1*. A homology search shows that the MAPO1-

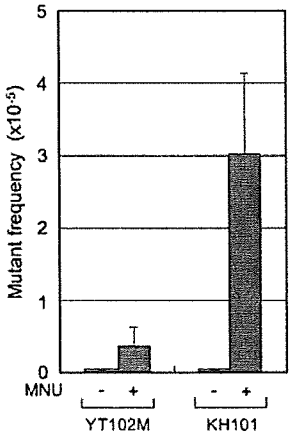

Figure 3 Elevated mutant frequency after *N*-methyl-*N*-nitrosourea (MNU) treatment. YT102M, a derivative from YT102 that stably expresses the human O^6-methylguanine-DNA methyltransferase (MGMT) protein, and KH101 cells were treated with or without 0.4 mM MNU. After the treatment, the number of viable cells and ouabain-resistant cells were determined, and the mutant frequencies were calculated. The mean values obtained from three experiments and the standard deviations (bars) are presented.

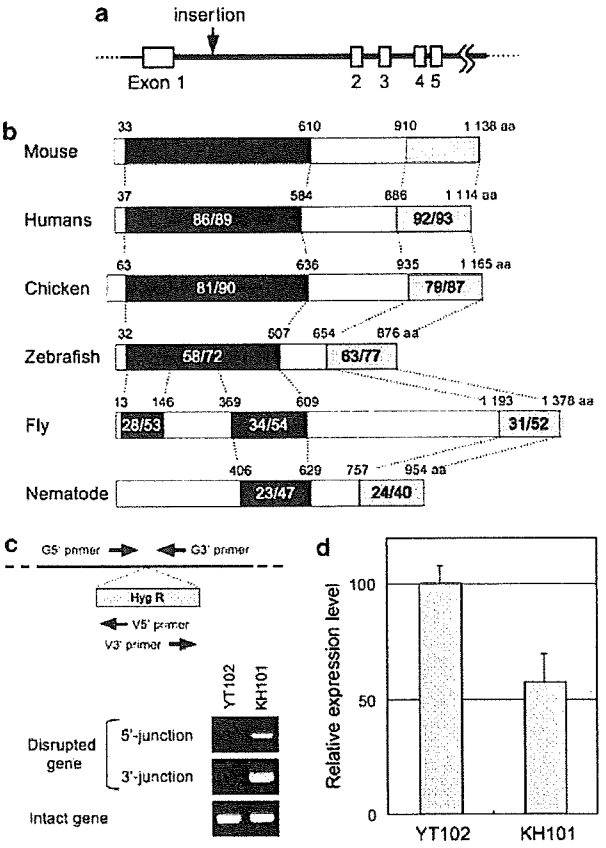

Figure 4 Structure and expression of the *Mapo1* gene. (**a**) A part of the gene in which the vector integration site is shown by an arrow. (**b**) Comparison of the MAPO1 proteins of various organisms. Accession numbers of the proteins are XP_912140 for mouse (*Mus musculus*), NP_065891 for humans (*Homo sapiens*), XP_420386 for chicken (*Gallus gallus*), XP_692808 for zebrafish (*Danio rerio*), NP_648943 for fly (*Drosophila melanogaster*) and NP_001023357 for nematode (*Caenorhabditis elegans*). The N- and C-terminal conserved regions, are shown by dark and light gray boxes, respectively. The numbers in the boxes indicate the percentages of amino acids showing identity/similarity in each conserved region of the proteins in comparison to those for mouse. The numbers above each box represent the amino-acid numbers beginning from the N-terminal ends of the proteins. (**c**) PCR analyses of the *Mapo1* gene in KH101 mutant cells. The upper panel shows the orientation and positions of four kinds of PCR primers designed for determination of the genomic and vector DNA sequences. The lower panel demonstrates the PCR-amplified 5′- and 3′-junctions of the wild-type and mutant forms of gene fragments. Amplified DNAs were separated by agarose gel electrophoresis and visualized by ethidium bromide staining. (**d**) The relative expression levels of the *Mapo1* gene as measured by quantitative real-time PCR.

related sequences are present in a wide range of multicellular organisms ranging from humans to nematode, but not found in microorganisms, including budding and fission yeasts. There are highly conserved sequences in the amino- and the carboxyl-terminal regions of the protein (Figure 4b).

To determine whether either a single or both allele(s) of the gene was disrupted in the mutant, we performed PCR analyses using two sets of primers specific for the disrupted gene, G5′ + V5′ and V3′ + G3′ primers, and a G5′ + G3′ primer set for the intact sequence of wild-type allele (Figure 4c). In the sample from the KH101 mutant, signals for the 5′- and 3′-junctions of the *Mapo1* gene and the vector DNA, and also a signal specific for the intact gene, were detected. In the sample derived from YT102, only a signal for the intact gene was found. These results suggest that one of the *Mapo1* alleles was disrupted, whereas the other remains intact in KH101 cells. In proportion to the gene dosage, the expression level of the *Mapo1* gene in KH101 ($Mapo1^{+/-}$) cells was approximately half the amount of that of YT102 ($Mapo1^{+/+}$) cells, as measured by quantitative real-time PCR (Figure 4d).

Suppression of the MAPO1 function by small interfering RNA

A synthetic small interfering RNA (siRNA) for the *Mapo1* gene, siMapo1, was introduced into YT102 cells and its expression level was determined 48 h later. An siRNA composed of a sequence unrelated to the *Mapo1* gene was also introduced as a control. The expression level of the *Mapo1* gene in siMapo1-treated cells was reduced to 43% of that of cells that received the control RNA, siCont (Figure 5a). These two types of cells were treated with or without 1 mM MNU and, after incubation for 2, 3 and 4 days, were subjected to flow cytometric analysis to monitor the appearance of cells with a sub-G1 DNA content. After treatment with MNU, the sub-G1 cell population increased gradually in cells treated with either type of siRNA, but the degree of increase in cells treated with siRNA for *Mapo1* was significantly lower than that obtained with control siRNA-treated cells (Figure 5b). A similar result was obtained by using siRNA that binds to a different region of *Mapo1* sequence (data not shown). Therefore, a good correlation was observed between the *Mapo1* expression level and the sub-G1 population in cell culture after MNU treatment. As an increase in the sub-G1 population represents the number of cells that undergo apoptotic cell death, these results suggest that the MAPO1 function is involved in O^6-methylguanine-induced apoptosis.

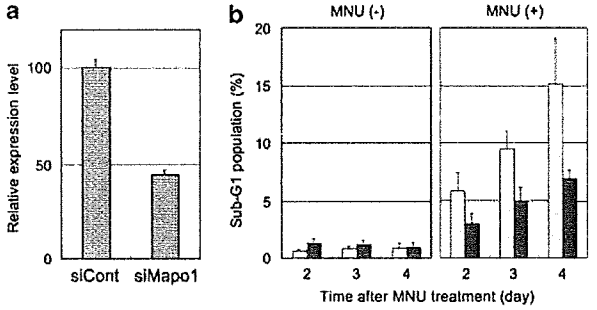

Figure 5 Suppression of apoptosis by small interfering RNA (siRNA) for *Mapo1*. (**a**) The expression levels of the *Mapo1* gene in YT102 ($Mgmt^{-/-}$) cells treated with control and *Mapo1* siRNA, as measured by real-time PCR. (**b**) Sub-G1 population in YT102 cells treated with control and *Mapo1* siRNA after *N*-methyl-*N*-nitrosourea (MNU) application. At 2 days after the application of either type of siRNA, YT102 cells were treated with or without 1 mM MNU for 1 h and then incubated for several days. At various times after MNU treatment, cells were harvested and subjected to a flow cytometric analysis. Light and dark columns represent sub-G1 population (%) for control siRNA- and *Mapo1* siRNA-treated cells, respectively.

Effects of Mapo1 *mutation on apoptosis-related events*

We analysed the levels of the phosphorylation of p53, CHK1 and histone H2AX (γH2AX), which are believed to be the downstream targets of ATR kinase, when the cells were treated with MNU (Cejka *et al*., 2003; Stojic *et al*., 2004). As shown in Figure 6a, the MNU-induced phosphorylation of these proteins was clearly observed,

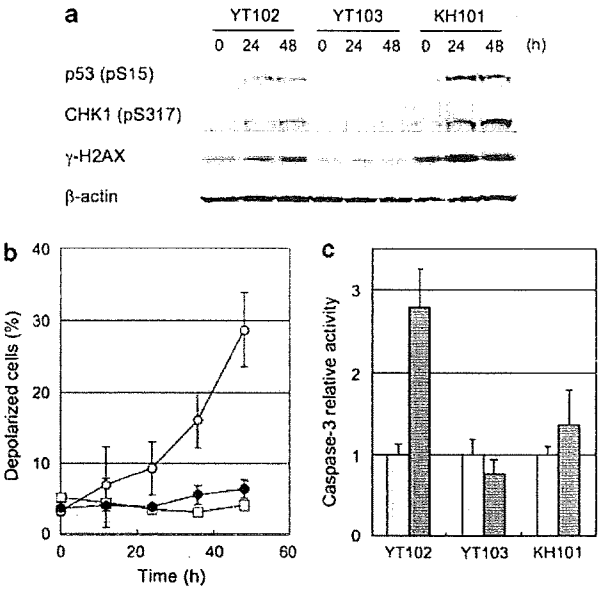

Figure 6 The expression of apoptosis-related activities in KH101 cells. (**a**) The activation of DNA damage signaling after exposure to *N*-methyl-*N*-nitrosourea (MNU). The phosphorylation of p53, CHK1 and histone H2AX was monitored by immunoblotting. β-Actin is a loading control. (**b**) Mitochondrial membrane depolarization after treatment with MNU. Cells were treated with 0.48 mM MNU for 1 h and further incubated. At the times indicated, cells were collected and applied to a mitochondrial membrane depolarization assay. The numbers of depolarized cells were counted by using a flow cytometer and the ratios were plotted. Open circles, YT102; open squares, YT103; closed circles, KH101. (**c**) Induction of caspase-3 activity after MNU treatment. Caspase-3 activity was determined at 72 h after treatment with or without 0.4 mM MNU. The values obtained with the MNU-treated cells were divided by those for the untreated cells, and the relative caspase-3 activities are shown. Light and dark columns represent the values for cells treated without and with MNU, respectively. All experiments were performed three times and the standard deviations are shown in bars.

after treatment with MNU, in KH101 as well as YT102 cells, although such phosphorylation was not shown in *Mlh1*-deficient YT103. These results indicate that the *Mapo1* mutation does not impair the MMR-dependent DNA damage detection and signaling.

We further examined the effect of *Mapo1* mutation on the depolarization of the mitochondrial membrane, which is known to occur during the process of apoptosis (Cossarizza *et al*., 1994). As expected, the depolarization of mitochondria is induced gradually in YT102 ($Mgmt^{-/-}$) cells after treatment with MNU (Figure 6b). However, no such depolarization was observed with KH101 ($Mgmt^{-/-}$ $Mapo1^{+/-}$) cells or with YT103 ($Mgmt^{-/-}$ $Mlh1^{-/-}$). To obtain further evidence that KH101 mutant cells are defective in a certain step in the process of apoptosis, we measured caspase-3 activity. Figure 6c shows levels of caspase-3 activity after treatment of the three types of cells with 0.4 mM MNU. Caspase-3 activity of YT102 cells increased three times the level of the untreated cells, whereas no increase was observed with YT103 cells. In KH101 cells, the level of caspase-3 activity after MNU treatment was as low as that of the untreated control. These results further support the notion that KH101 cells might have a defect in a certain step of the O^6-methylguanine-induced apoptosis pathway.

Cytoplasmic localization of EGFP-fused MAPO1 proteins

To analyse the subcellular localization of the MAPO1 protein, we have cloned the full-length mouse *Mapo1* cDNA and expressed EGFP-fused mMAPO1 protein in YT102 cells. As shown in Figure 7a, transiently expressed mMAPO1 protein is predominantly present in the cytoplasm. The cytoplasmic localization of mMAPO1 protein did not dramatically change even after treatment of cells with MNU. To assess whether this is the case for the highly conserved human ortholog, we also obtained the human cDNA for the gene and expressed EGFP-fused hMAPO1 protein in HeLa MR cells (Figure 7b). Similarly, the cytoplasmic localization of hMAPO1 was observed and it was found to be unaffected by the MNU treatment.

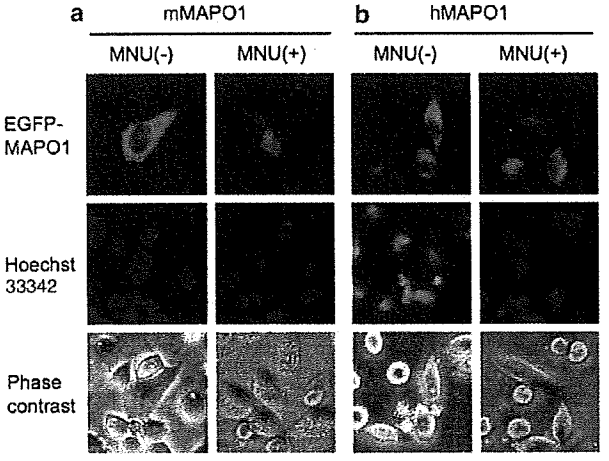

Figure 7 Cytoplasmic localization of MAPO1 proteins. The plasmid DNAs expressing EGFP-fused mouse and human MAPO1 proteins were transfected into YT102 and HeLa MR, respectively. After 24 h, the cells were treated with or without 0.4 mM *N*-methyl-*N*-nitrosourea (MNU) for 1 h. After another 24 h incubation, the cells were washed with phosphate-buffered saline (PBS) and stained with 10 μM of Hoechst33342 followed by the analyses using fluorescent microscopy. The images for EGFP-fused MAPO1, Hoechst33342 signals and phase contrast are represented at the top, middle and bottom, respectively. (a) Images of cells expressing EGFP-fused mMAPO1. (b) Images of cells expressing EGFP-fused hMAPO1.

Discussion

There are two distinct types of DNA lesions that induce apoptosis: modified bases that cause base mispairing and bulky DNA lesions that block DNA replication. The former requires MMR proteins for induction of apoptosis, whereas the latter induces apoptosis even without the function of such proteins. O^6-Methylguanine, produced in DNA by the action of simple alkylating agents, does not prevent the progression of DNA replication forks and apparently represents the former class DNA lesion (Singer *et al*., 1989; Haracska *et al*., 2000). During DNA replication, O^6-methylguanine (O^6-meG) can pair with thymine as well as cytosine, and unless repaired, the resulting O^6-meG:T mispair would lead to mutations after next round of replication. To suppress such an outcome, organisms have been equipped with a mechanism for eliminating cells carrying mutation-evoking DNA lesions. The MMR protein complex apparently acts as a molecular device to detect such lesions. The MutSα, consisting of MSH2 and MSH6, and PCNA complex first recognizes O^6-meG:T mispair in DNA and then MutLα, composed of MLH1 and PMS2, binds to the initial complex. The formation of the mismatch recognition complex is indispensable for the activation of DNA damage signaling as well as the induction of apoptosis (Hidaka *et al*., 2005; Yoshioka *et al*., 2006; Sanada *et al*., 2007).

The precise molecular mechanism of signal transduction downstream of mismatch recognition still remains to be determined. As many proteins would be involved in this process, we have initiated the present study to identify such proteins by gene-trap mutagenesis screening. As a selectable marker for the gene trap, a promoterless hygromycin B resistance gene placed near a splicing acceptor and an IRES sequences was used. This allowed efficient expression of the marker, when it was integrated into any region of actively transcribed genes to be mutated. Among Hyg^r cells selected, candidate clones could be obtained that might have defects in an apoptosis-related process. In this way, we were able to identify *Mapo1*, which turned out to be a novel gene involved in O^6-methylguanine-induced apoptosis. The *Mapo1* encodes a protein with a molecular mass of 125.6 kDa, carrying no characteristic functional motifs. The MAPO1 sequence, however, has the highly conserved amino- and carboxyl-terminal domains present in various multicellular organisms

ranging from humans to nematode, but not in microorganisms including yeast. This evolutional conservation might reflect its possible biological significance on the apoptosis in multicellular organisms.

In the present study, we show that *Mapo1* mutation renders the cells significantly resistant to MNU, although it does not dramatically affect its sensitivity to the killing effect caused by MMS, ACNU, etoposide or UV irradiation (Figure 2). Importantly, even when the *Mapo1*-defective KH101 cells are treated with MNU, the depolarization of the mitochondrial membrane and caspase-3 activation, hallmarks of apoptosis induction, are significantly suppressed. As the phosphorylation of p53, CHK1 and histone H2AX, downstream targets of ATR kinase, is nevertheless observed in KH101 cells after MNU treatment (Figure 6), the MAPO1 protein, which is localized in the cytoplasm (Figure 7), is not likely to be involved in the nuclear translocation of MutSα complex (Christmann and Kaina, 2000) nor in the activation of MNU-induced DNA damage signaling. These results suggest that MAPO1 may play a role in a certain step(s) of the signal-transduction pathway of apoptosis, induced by the O^6-methylguanine, that would activate the apoptotic function of the mitochondria.

It is remarkable that the *Mapo1* mutation exerts its effect even when one of the alleles is intact. KH101 (*Mgmt*$^{-/-}$*Mapo1*$^{+/-}$) cells exhibit a significantly higher level of resistance to MNU than YT102 (*Mgmt*$^{-/-}$*Mapo1*$^{+/+}$) cells. We have also shown that MNU-induced apoptosis, as measured by an increase in the sub-G1 population, is significantly suppressed when the expression level of *Mapo1* is reduced to half its normal level by siRNA treatment. This haploinsufficient character of the *Mapo1* gene is reminiscent of the phenomenon observed with MMR-related genes. *Mgmt*$^{-/-}$*Mlh1*$^{+/-}$ cells, which carry almost half the amount of MLH1 protein in comparison with *Mlh1*$^{+/+}$ cells, are substantially resistant to the killing action of MNU than are *Mgmt*$^{-/-}$*Mlh1*$^{+/+}$ cells (Kawate *et al*., 2000; Cejka *et al*., 2003; Takagi *et al*., 2003). This haploinsufficient nature may be related to the fact that MLH1 protein forms a heterodimer with PMS2 to form a MutLα complex (Li and Modrich, 1995). MutLα further binds to MutSα, which is composed of MSH2 and MSH6, and participates in the recognition of mismatch bases in DNA to initiate the apoptotic reaction. Thus, these mismatch recognition proteins act in a stoichiometric manner, rather than in a catalytic one, in inducing the apoptotic signal. As the *Mapo1* exhibits a similar phenotype, it may exert its function by forming a complex with other components, rather than by acting in a catalytic manner or by changing the localization of the protein.

To obtain further insight into the *Mapo1* function, it is necessary to establish a cell line defective in both of the alleles of the gene. The neomycin selection method, which is usually used to isolate such clones, cannot be applied to the present study, as the neomycin-resistant marker was already introduced into the parental strain to knockout the *Mgmt* gene. Other strategies are now being applied to isolate such doubly deficient cells that might show a higher level of resistance to the MNU treatment.

Materials and methods

Cell lines and cell culture

YT102 (*Mgmt*$^{-/-}$*Mlh1*$^{+/+}$) and YT103 (*Mgmt*$^{-/-}$*Mlh1*$^{-/-}$) are cell lines established, by expressing SV40 T antigen, from primary cells consisting of fibroblasts derived from the lung tissue of *Mgmt* and *Mgmt Mlh1*-knockout mice, respectively (Takagi *et al*., 2003). YT102M is a derivative of YT102 that carries the expression vector, pIREShyg2:*Mgmt* (Takagi *et al*., 2003), to stably express human MGMT. The cells were cultivated in Dulbecco's modified Eagle's medium supplemented with 10% fetal bovine serum (FBS) at 37 °C in 5% CO_2.

Gene-trap mutagenesis and screening for MNU^r *clones*

The retrovirus vector, pLHΔU3L, which carries the hygromycin B resistance gene, was constructed for the gene-trap mutagenesis. The promoter region in 3′LTR of a retroviral vector, pDON-AI (Takara Bio Inc., Ohtsu, Japan), was removed by *Aff*II and *Xba*I digestion followed by self-ligation. The SV40 promoter and the neomycin resistance gene were removed from the vector by digestion with *Sal*I and *Xho*I, and then the loxP^2-containing fragment, which was excised from the pBS246 vector (Invitrogen, Carlsbad, CA, USA) by *Not*I digestion, was inserted into the site after blunt ending. A DNA fragment containing synthetic intron (IVS), IRES, hygromycin B resistance gene and poly A signal sequences was isolated from pIREShyg2 vector (Clontech, Mountain View, CA, USA), and then inserted into the *Eco*RV site in the loxP^2 region of the retroviral vector. The resulting pLHΔU3L vector was introduced into ΨMP34 (Takara Bio Inc.) cells by using Lipofectamine 2000 (Invitrogen) according to the manufacturer's instructions. After incubation of the cells for 1.5 days at 33 °C, the retroviral particles carrying the gene-trap construct in the medium were recovered and filtered.

Approximately 1.5×10^7 of YT102 cells grown on twenty 10-cm dishes were infected with the retrovirus and incubated for 15 h. The cells were further cultivated in a virus-free fresh medium for another day and then selected in a medium containing 0.6 mg/ml of hygromycin B for 55 h. After washing with phosphate-buffered saline (PBS) three times, the cells were treated with 0.4 mM MNU in serum-free medium for 1 h and further incubated in complete medium containing 10% FBS. Colonies formed were subjected to a quantitative cell survival assay with various concentrations of MNU. Finally, MNU^r mutant cell lines were thus obtained.

Immunoblotting

Whole cell extracts were prepared by the lyses of cells with 2 × SDS–polyacrylamide gel electrophoresis (PAGE) sample buffer (120 mM Tris–HCl (pH 6.8), 4% SDS, 20% glycerol, 200 mM dithiothreitol and 0.002% bromophenol blue) and then subjected to SDS–PAGE and electroblotted onto a PVDF membrane (Bio-Rad, Hercules, CA, USA). Detection was performed using an ECL Plus or Advance western blotting detection kit (GE Healthcare, Buckinghamshire, UK). The primary antibodies used were: anti-MGMT (BD Pharmingen, San Diego, CA, USA), anti-MSH2 (Zymed, San Francisco, CA, USA), anti-MSH6 (BD Transduction, San Jose, CA, USA), anti-MLH1 (Santa Cruz, Santa Cruz, CA, USA), anti-PMS2 (BD Pharmingen), anti-β-actin (Sigma, St Louis, MO, USA), anti-phospho-p53 (Ser15) (Cell Signaling, Danvers, MA, USA), anti-phospho-CHK1 (Ser317) (Bethyl, Montgomery, TX, USA) and anti-phospho-histone H2AX (Ser139) (Upstate, Temecula, CA, USA).

Survival of cells treated with MNU, MMS, ACNU etoposide and UV-C
The cells were treated with various concentrations of MNU, MMS or ACNU in serum-free medium for 1 h, etoposide in a medium containing 10% FBS for 12 h, or irradiated with different doses of UV-C. After cultivation with a medium containing 10% FBS for 6 days, the number of colonies was counted and the survival rate was calculated.

Measurement of mutant frequency
The cells were treated with 0 or 0.4 mM MNU as described above and incubated for 4 days. Then, the cells were placed in a medium containing 2 mM ouabain for 10 days. After staining, the number of resistant colonies was counted. In parallel, a cell suspension containing about 500 cells was seeded in several dishes and the number of viable cells was counted.

Analyses of the disrupted gene by PCR
For inverse PCR, 10 μg of genomic DNA prepared from KH101 mutant cells was digested with *Bam*HI and *Bgl*II, or *Hin*dII restriction enzymes. Precipitated DNA was resuspended in 1 ml of buffer (66 mM Tris–HCl; pH 7.6, 6.6 mM $MgCl_2$, 10 mM dithiothreitol and 0.1 mM ATP) and incubated at 16 °C overnight after adding 1750 U of T4 DNA ligase (Takara Bio Inc.). By using the DNA as a template, 5′- and 3′-junctions between the disrupted gene and the vector DNA were amplified by PCR with two primer sets designed for the vector sequence, GS1: 5′-AGCTTACCTCCCGGTGGTGGG TCGGTGGTC-3′ and DON1: 5′-GCGGGGGCGACTTCG GCTCACAGCGCGCCC-3′ or US1: 5′-CTTGTGGTCTCG CTGTTCCTTGGGAGGGTC–3′ and UR1: 5′-GGGGCACC CTGGAAACATCTGATGGTTCTC–3′, respectively. The DNA fragments amplified were cloned into a pGEM-Teasy vector (Promega, Madison, WI, USA). The nucleotide sequences of the clones were determined and analysed in NCBI GenBank.

For the detection of the mutant allele, DNA fragments specific for the disrupted *Mapo1* gene or for the intact gene were amplified by PCR, using primer sets, G5′ + V5′ and V3′ + G3′, or G5′ + G3′, respectively. The nucleotide sequences of PCR primers are G5′, 5′-ATGCTAAAGTAGCTT GTTGTGGGCCTTTCC-3′; G3′, 5′-CGCTCATACAAGCA GTTAGCAACCGC-3′; V5′, 5′-ATTTAGTCTCCAGAAAA AGGGGGGAATG-3′ and V3′, 5′-AGCTTACCTCCCGGT GGTGGGTCGGTGGTC-3′.

Measurement of gene expression by real-time PCR
Total RNA was prepared from cells grown on a six-well plate using the RNeasy Mini kit (Qiagen, Hilden, Germany) and were used to synthesize cDNAs by using PrimeScript Reverse Transcriptase (Takara Bio Inc.). Real-time PCR was performed with a light cycler (Roche, Mannheim, Germany) using SYBR Premix Ex Taq (Takara Bio Inc.). The PCR primers for a *Mapo1* gene, pMapo1-F and pMapo1-R, and for a *Gapdh* gene as a reference, pmGapdh-F and pmGapdh-R, were purchased from Takara Bio Inc. and the nucleotide sequences are pMapo1-F, 5′-GCACACAGCACACCTGTTGA-3′; pMapo1-R, 5′-GCGCTGGTAACTGCTGGAA-3′; pmGapdh-F, 5′-AAATGGTGAAGGTCGGTGTG-3′; pmGapdh-R, 5′-TGA AGGGGTCGTTGATGG-3′.

siRNA transfection
Stealth RNAi for the *Mapo1* sequence (siMapo1), 5′-CA GAAAGCAGAGGATGTTCCTATTA-3′, was purchased from Invitrogen. After culturing 1×10^5 cells in a six-well plate for 1 day, the cells were transfected with 20 nM siRNA, using the Lipofectamine RNAiMAX reagent (Invitrogen) according to the manufacturer's protocol. For the control transfection, Stealth RNAi Negative Control Medium GC Duplex (Invitrogen) was used.

Mitochondrial membrane depolarization assay
About 2×10^5 cells were washed with PBS and treated with 0.48 mM MNU for 1 h. The doses of the drugs correspond to six lethal hits for YT102 cells, as calculated from the survival curves. The cells were further incubated in complete medium and collected at 0, 12, 24, 36 and 48 h after the treatment with MNU. The mitochondrial membrane potential assay was performed using the MitoProbe DiOC2(3) Assay kit (Invitrogen), as described earlier (Takagi *et al.*, 2008).

Molecular cloning of Mapo1 *cDNAs*
To clone mouse *Mapo1* cDNA, RT–PCR reactions were carried out to amplify four parts of cDNA with overlapping sequences using cDNAs, synthesized from total RNA prepared from YT102 cells, as templates. The four cDNA fragments were connected to each other at the internal restriction sites and the full-length mouse *Mapo1* cDNA was thus generated. The human *Mapo1* cDNA (KIAA1450) was obtained from the Kazusa DNA Research Institute (Kisarazu, Japan).

Expression of EGFP-fused MAPO1 protein and microscopic analysis
To construct plasmids to express MAPO1 proteins fused with EGFP at the C-terminal regions, we introduced mouse and human *Mapo1* cDNA together with the EGFP gene into *Eco*RV and *Not*I site of pIRESpuro2 (Clontech) plasmid. To express the EGFP-fused MAPO1 proteins, 0.8 μg of plasmid DNAs was transfected using Lipofectamine 2000 into YT102 (for mouse) or HeLa MR (for humans) cells growing in 24-well plates according to the manufacturer's instructions. The cells were treated with or without 0.4 mM MNU for 1 h at 24 h after transfection. After another 24-h incubation, the cells were washed with PBS and stained with 10 μM of Hoechst33342 (Invitrogen) and fluorescent signals were observed by fluorescent microscopy (Nikon, Tokyo, Japan).

Other methods
Flow cytometric analysis and of caspase-3 activity assay were performed as described earlier (Hidaka *et al.*, 2005).

Acknowledgements

We thank the Kazusa DNA Research Institute for providing hKIAA1450 cDNA. This study was supported by grants (including a Frontier Research Grant) from the Ministry of Education, Culture, Sports, Science and Technology of Japan.

Conflict of interest

The authors declare no conflict of interest.

References

Beranek DT. (1990). Distribution of methyl and ethyl adducts following alkylation with monofunctional alkylating agents. *Mutat Res* **231**: 11–30.

Branch P, Aquilina G, Bignami M, Karran P. (1993). Defective mismatch binding and a mutator phenotype in cells tolerant to DNA damage. *Nature* **362**: 652–654.

Caporali S, Falcinelli S, Starace G, Russo MT, Bonmassar E, Jiricny J *et al.* (2004). DNA damage induced by temozolomide signals to both ATM and ATR: role of the mismatch repair system. *Mol Pharmacol* **66**: 478–491.

Cejka P, Stojic L, Mojas N, Russell AM, Heinimann K, Cannavo E *et al.* (2003). Methylation-induced G(2)/M arrest requires a full complement of the mismatch repair protein hMLH1. *EMBO J* **22**: 2245–2254.

Christmann M, Kaina B. (2000). Nuclear translocation of mismatch repair proteins MSH2 and MSH6 as a response of cells to alkylating agents. *J Biol Chem* **275**: 36256–36262.

Cossarizza A, Kalashnikova G, Grassilli E, Chiappelli F, Salvioli S, Capri M *et al.* (1994). Mitochondrial modifications during rat thymocyte apoptosis: a study at the single cell level. *Exp Cell Res* **214**: 323–330.

Coulondre C, Miller JH. (1977). Genetic studies of the lac repressor. IV. Mutagenic specificity in the lacI gene of *Escherichia coli*. *J Mol Biol* **117**: 577–606.

Fishel R. (1998). Mismatch repair, molecular switches, and signal transduction. *Genes Dev* **12**: 2096–2101.

Glaab WE, Risinger JI, Umar A, Barrett JC, Kunkel TA, Tindall KR. (1998). Cellular resistance and hypermutability in mismatch repair-deficient human cancer cell lines following treatment with methyl methanesulfonate. *Mutat Res* **398**: 197–207.

Glassner BJ, Weeda G, Allan JM, Broekhof JL, Carls NH, Donker I *et al.* (1999). DNA repair methyltransferase (Mgmt) knockout mice are sensitive to the lethal effects of chemotherapeutic alkylating agents. *Mutagenesis* **14**: 339–347.

Guo G, Wang W, Bradley A. (2004). Mismatch repair genes identified using genetic screens in Blm-deficient embryonic stem cells. *Nature* **429**: 891–985.

Haracska L, Prakash S, Prakash L. (2000). Replication past O^6-methylguanine by yeast and human DNA polymerase eta. *Mol Cell Biol* **20**: 8001–8007.

Hickman MJ, Samson LD. (1999). Role of DNA mismatch repair and p53 in signaling induction of apoptosis by alkylating agents. *Proc Natl Acad Sci USA* **96**: 10764–10769.

Hickman MJ, Samson LD. (2004). Apoptotic signaling in response to a single type of DNA lesion, O^6-methylguanine. *Mol Cell* **14**: 105–116.

Hidaka M, Takagi Y, Takano TY, Sekiguchi M. (2005). PCNA-MutSalpha-mediated binding of MutLalpha to replicative DNA with mismatched bases to induce apoptosis in human cells. *Nucleic Acids Res* **33**: 5703–5712.

Ishida Y, Leder P. (1999). RET: a poly A-trap retrovirus vector for reversible disruption and expression monitoring of genes in living cells. *Nucleic Acids Res* **27**: e35.

Ito T, Nakamura T, Maki H, Sekiguchi M. (1994). Roles of transcription and repair in alkylation mutagenesis. *Mutat Res* **314**: 273–285.

Kaina B, Christmann M, Naumann S, Roos WP. (2007). MGMT: key node in the battle against genotoxicity, carcinogenicity and apoptosis induced by alkylating agents. *DNA Repair (Amst)* **6**: 1079–1099.

Kaina B, Fritz G, Mitra S, Coquerelle T. (1991). Transfection and expression of human O^6-methylguanine-DNA methyltransferase (MGMT) cDNA in Chinese hamster cells: the role of MGMT in protection against the genotoxic effects of alkylating agents. *Carcinogenesis* **12**: 1857–1867.

Karran P. (2001). Mechanisms of tolerance to DNA damaging therapeutic drugs. *Carcinogenesis* **22**: 1931–1937.

Kat A, Thilly WG, Fang WH, Longley MJ, Li GM, Modrich P. (1993). An alkylation-tolerant, mutator human cell line is deficient in strand-specific mismatch repair. *Proc Natl Acad Sci USA* **90**: 6424–6428.

Kawate H, Itoh R, Sakumi K, Nakabeppu Y, Tsuzuki T, Ide F *et al.* (2000). A defect in a single allele of the Mlh1 gene causes dissociation of the killing and tumorigenic actions of an alkylating carcinogen in methyltransferase-deficient mice. *Carcinogenesis* **21**: 301–305.

Kawate H, Sakumi K, Tsuzuki T, Nakatsuru Y, Ishikawa T, Takahashi S *et al.* (1998). Separation of killing and tumorigenic effects of an alkylating agent in mice defective in two of the DNA repair genes. *Proc Natl Acad Sci USA* **95**: 5116–5120.

Li G, Modrich P. (1995). Restoration of mismatch repair to nuclear extracts of H6 colorectal tumor cells by a heterodimer of human MutL homologs. *Proc Natl Acad Sci USA* **92**: 1950–1954.

Loechler EL, Green CL, Essigmann JM. (1984). *In vivo* mutagenesis by O^6-methylguanine built into a unique site in a viral genome. *Proc Natl Acad Sci USA* **81**: 6271–6275.

Margison GP, Santibanez-Koref MF. (2002). O^6-alkylguanine-DNA alkyltransferase: role in carcinogenesis and chemotherapy. *Bioessays* **24**: 255–266.

Meikrantz W, Bergom MA, Memisoglu A, Samson L. (1998). O^6-alkylguanine DNA lesions trigger apoptosis. *Carcinogenesis* **19**: 369–372.

Ochs K, Kaina B. (2000). Apoptosis induced by DNA damage O^6-methylguanine is Bcl-2 and caspase-9/3 regulated and Fas/caspase-8 independent. *Cancer Res* **60**: 5815–5824.

Pegg AE. (2000). Repair of O(6)-alkylguanine by alkyltransferases. *Mutat Res* **462**: 83–100.

Peng M, Litman R, Xie J, Sharma S, Brosh Jr RM, Cantor SB. (2007). The FANCJ/MutLalpha interaction is required for correction of the cross-link response in FA-J cells. *EMBO J* **26**: 3238–3249.

Pepponi R, Marra G, Fuggetta MP, Falcinelli S, Pagani E, Bonmassar E *et al.* (2003). The effect of O^6-alkylguanine-DNA alkyltransferase and mismatch repair activities on the sensitivity of human melanoma cells to temozolomide, 1,3-bis(2-chloroethyl)1-nitrosourea, and cisplatin. *J Pharmacol Exp Ther* **304**: 661–668.

Sakumi K, Shiraishi A, Shimizu S, Tsuzuki T, Ishikawa T, Sekiguchi M. (1997). Methylnitrosourea-induced tumorigenesis in MGMT gene knockout mice. *Cancer Res* **57**: 2415–2418.

Sanada M, Hidaka M, Takagi Y, Takano TY, Nakatsu Y, Tsuzuki T *et al.* (2007). Modes of actions of two types of anti-neoplastic drugs, dacarbazine and ACNU, to induce apoptosis. *Carcinogenesis* **28**: 2657–2663.

Singer B, Chavez F, Goodman MF, Essigmann JM, Dosanjh MK. (1989). Effect of 3′ flanking neighbors on kinetics of pairing of dCTP or dTTP opposite O^6-methylguanine in a defined primed oligonucleotide when *Escherichia coli* DNA polymerase I is used. *Proc Natl Acad Sci USA* **86**: 8271–8274.

Stojic L, Mojas N, Cejka P, Di Pietro M, Ferrari S, Marra G *et al.* (2004). Mismatch repair-dependent G2 checkpoint induced by low doses of SN1 type methylating agents requires the ATR kinase. *Genes Dev* **18**: 1331–1344.

Takagi Y, Hidaka M, Sanada M, Yoshida H, Sekiguchi M. (2008). Different initial steps of apoptosis induced by two types of antineoplastic drugs. *Biochem Pharmacol* **76**: 303–311.

Takagi Y, Takahashi M, Sanada M, Ito R, Yamaizumi M, Sekiguchi M. (2003). Roles of MGMT and MLH1 proteins in alkylation-induced apoptosis and mutagenesis. *DNA Repair (Amst)* **2**: 1135–1146.

Tominaga Y, Tsuzuki T, Shiraishi A, Kawate H, Sekiguchi M. (1997). Alkylation-induced apoptosis of embryonic stem cells in which the gene for DNA-repair, methyltransferase, had been disrupted by gene targeting. *Carcinogenesis* **18**: 889–896.

Tsuzuki T, Sakumi K, Shiraishi A, Kawate H, Igarashi H, Iwakuma T *et al.* (1996). Targeted disruption of the DNA repair methyltransferase gene renders mice hypersensitive to alkylating agent. *Carcinogenesis* **17**: 1215–1220.

Wiles MV, Vauti F, Otte J, Fuchtbauer EM, Ruiz P, Fuchtbauer A *et al.* (2000). Establishment of a gene-trap sequence tag library to generate mutant mice from embryonic stem cells. *Nat Genet* **24**: 13–14.

Yoshioka K, Yoshioka Y, Hsieh P. (2006). ATR kinase activation mediated by MutSalpha and MutLalpha in response to cytotoxic O^6-methylguanine adducts. *Mol Cell* **22**: 501–510.